Effectiveness-Mass Transfer Units (ε-MTU) Model of a Reverse Osmosis Membrane Mass Exchanger

Leonardo D. Banchik[1], Mostafa H. Sharqawy[2], John H. Lienhard V[*, 1]

[1] Department of Mechanical Engineering, Massachusetts Institute of Technology, Cambridge, MA 02139-4307, USA
[2] Department of Mechanical Engineering, King Fahd University of Petroleum and Minerals, Dhahran 31261, Saudi Arabia

---

Abstract

A strong analogy exists between heat exchangers and osmotic mass exchangers. The effectiveness - number of transfer units (ε-NTU) method is well-known for the sizing and rating of heat exchangers. A similar method, called the effectiveness - mass transfer units (ε-MTU) method, is developed for reverse osmosis (RO) mass exchangers. Governing equations for an RO mass exchanger are nondimensionalized assuming ideal membrane characteristics and a linearized form of the osmotic pressure function for seawater. A closed form solution is found which relates three dimensionless groups: the number of mass transfer units, which is an effective size of the exchanger; a pressure ratio, which relates osmotic and hydraulic pressures; and the recovery ratio, which is the ratio of permeate to inlet feed flow rates. A novel performance parameter, the effectiveness of an RO exchanger, is defined as a ratio of the recovery ratio to the maximum recovery ratio. A one-dimensional numerical model is developed to correct for the effects of feed-side external concentration polarization and nonlinearities in osmotic pressure as a function of salinity. A comparison of model results to experimental data found in the literature resulted in an average error of less than 7.8%. The analytical ε-MTU model can be used for design or performance evaluation of RO membrane mass exchangers.

Keywords: Mass exchanger, reverse osmosis, seawater, desalination, effectiveness, mass transfer units, concentration polarization, heat and mass transfer similarity

[*] Corresponding author
Email address: lienhard@mit.edu (John H. Lienhard)
Phone: +1-617-253-3790

Nomenclature

A	water permeability coefficient	kg m^{-2} s^{-1} kPa^{-1}
A_m	total membrane surface area	m^2
b	molality – moles of solutes per kilogram of solvent	mol kg^{-1}
C	modified van 't Hoff coefficient	kPa kg g^{-1}
c	molarity - moles of the solute per cubic meter of solvent	mol m^{-3}
D	mass diffusivity	m^2 s^{-1}
h	half feed channel height	m
i	the van 't Hoff factor	
k	mass transfer coefficient	m s^{-1}
M	molar mass	kg mol^{-1}
$\dot{m}$	mass flow rate	kg s^{-1}
P	pressure	kPa
R	ideal gas constant	kJ mol^{-1} K^{-1}
Re	Reynolds number	
Sc	Schmidt number	
T	temperature	°C or K
w	salinity - grams of solutes per kilogram of solution	g kg^{-1}

Greek symbols

β	correction factor for concentration polarization and nonlinearity in osmotic pressure	
ε	effectiveness	
κ	constant for determining osmotic coefficient (Eq. A.8)	
λ	constant for determining osmotic coefficient (Eq. A.8)	
π	osmotic pressure	kPa
ρ	density	kg m^{-3}
ϕ	osmotic coefficient	
ν	kinematic viscosity	m^2 s^{-1}
ω	Lambert or omega function	

Subscripts

c	cold
f	feed
h	hot
in	inlet
j	j^{th} solute in a solution
max	maximum

out	outlet	
p	permeate	
pure	refers to pure water	
recipe	corresponds to a reference of seawater constituents	
s	salt	
sat	saturated state	

Superscripts

’	modified value	
’’	per unit area, flux	m^{-2}

Abbreviations

CP	concentration polarization
MTU	number of mass transfer units
NTU	number of transfer units
RO	reverse osmosis
RR	recovery ratio
SR	osmotic pressure ratio

Introduction

Many transport theories have been developed for reverse osmosis (RO) which describe the local transport of the pure water and solutes through a zero-dimensional membrane. However, because the feed stream becomes more concentrated along the length of the membrane, the local driving potential for water flux changes along the length as well. This indicates that the driving potential should be integrated over the membrane area in the streamwise dimension to more accurately determine the performance of the RO exchanger.

Mathematical models for the mass transport process through RO membranes have been developed and reviewed in detail in the literature [1-11]. These models can be divided into three main groups: the irreversible thermodynamic models, where the local fluxes of solute and solvent are related to the chemical potential differences across the membrane [12-14]; the porous flow model, which assumes that water both diffuses and advects through the membrane pores [1, 15, 16]; and the solution-diffusion model, which assumes that both water and solutes diffuse between the interstitial spaces of the membrane polymer chains [11, 17, 18].

The solution-diffusion model, developed by Lonsdale, Merten, and Riley in 1965 [17], is one of the most useful models despite its simplicity and some drawbacks that have been discussed elsewhere [6, 18, 19]. Much research has been conducted on the physics of the solution-diffusion model [7, 18, 20-22] and many numerical studies have been applied to account for the more complex effects of concentration polarization, salt diffusion, and fouling [23-27]. Other studies have applied the solution-diffusion model

for the design of RO modules such as spiral wound, hollow fiber, and crossflow long channels [25, 28-33]. The solution-diffusion model has also been used together with relevant conservation laws to optimize the operation of RO systems and minimize the specific power consumption and cost of a plant [34-43].

Song and Tay [33] developed an analytical model of an RO exchanger based on the solution-diffusion model for transport across the membrane and conservation laws for a crossflow configuration; osmotic pressure was linearized, zero salt passage assumed, and hydraulic losses were neglected. They found good agreement with experiments that they performed as well. The present work builds from a similar approach, but organizes the dimensional analysis into a clear framework that is analogous to that used for heat exchanger rating and design as has been done for other osmotic mass exchangers [44]. Additionally, the present formulation better separates the physical variables and considers the effects of concentration polarization and the nonlinearity in osmotic pressure, both of which become significant when considering feed waters that are more saline than brackish water. Finally, the model is compared to a number of published datasets.

1. Analogy to a Heat Exchanger

An RO mass exchanger is a single-stream osmotic mass exchanger and is analogous to a single-stream heat exchanger. A single-stream exchanger is one in which the temperature or osmotic pressure of only one stream changes in the exchanger. In the heat exchanger shown in Fig. 1a, the temperature difference between hot steam and cold fluid is the driving potential for a differential amount of heat transfer. The resistance to heat flow per unit area is the reciprocal of the overall heat transfer coefficient, U. The

exchanger shown here has a fixed hot-side temperature throughout the length of the exchanger, e.g., as it might in a condensation process.

The analogous system for an osmotic mass exchanger is the RO system shown in Fig. 1b. A saline feed solution with an osmotic pressure and a fixed high hydraulic pressure enters the left side of the exchanger. Along the length of the exchanger, permeate is forced through an ideal (zero salt passage) semi-permeable membrane, leaving the salts behind. At the exit of the exchanger, the feed is recovered as concentrated brine and the product is recovered as the accumulated amount of pure permeate. The driving potential for mass transfer is the difference in hydraulic and osmotic pressures. The resistance to the mass transfer per unit area is the reciprocal of the water permeability coefficient, A.

In heat exchangers, the effectiveness - number of transfer units (ε-NTU) method developed by Kays and London [45] is a well-known design tool which can either determine the required surface area of a heat exchanger for a fixed effectiveness and inlet conditions or determine the performance of the exchanger given the operating conditions and surface area. The method uses three dimensionless groups: the effectiveness, which is the ratio of actual heat exchange to the maximum heat exchange possible; a heat capacity rate ratio, which is the heat capacity rate of the minimum capacity rate stream divided by that of the maximum capacity rate stream; and the number of transfer units, which is an effective size of the heat exchanger. This paper develops an effectiveness - mass transfer units (ε-MTU) method for a crossflow reverse osmosis mass exchanger.

2. Analytical Model for an RO Mass Exchanger

Figure 2 is a schematic drawing of a crossflow osmotic mass exchanger operating in the RO mode. A feed solution with a high salt concentration flows through a channel alongside a semi-permeable membrane. The bulk hydraulic pressure difference (ΔP) is greater than the bulk osmotic pressure difference ($\Delta\pi$) across the membrane, so that water flows from the feed side to the permeate side. The inlet conditions of the feed stream are given as the mass flow rate, hydraulic pressure, and osmotic pressure (which is a function of the local stream salinity in the bulk) as indicated in Fig. 2. The total membrane area A_m and water permeability coefficient A of the membrane material are also given. The model makes the following assumptions:

- The water permeability coefficient (A) is constant and is independent of inlet feed salinity.
- Concentration polarization (CP) effects are incorporated via use of a dimensionless correction factor.
- Hydraulic pressure drop along the length of each flow channel is negligible, so that the applied pressure difference between the channels remains constant.
- Salt rejection is 100%, so that only pure water diffuses through the membrane. This is a reasonable assumption when one considers the high salt rejection currently found in commercial RO membranes [46].
- The osmotic pressure of a stream follows van 't Hoff's equation so that it is linearly proportional to the local feed-side salt concentration.[2]

[2] Nonlinearities are ignored in the initial development but are then included in a subsequent section as part of a more rigorous analysis.

The permeate flow rate through a differential area of membrane is given by:

$$d\dot{m}_p = A(\Delta P - \beta\Delta\pi)dA_m \quad (1)$$

where $\dot{m}_p$ is the permeate mass flow rate through the membrane [kg/s]; A is the mass-based water permeability coefficient[3] of the membrane [kg/m^2-s-kPa]; ΔP is the bulk hydraulic pressure difference between the feed and permeate ($P_f - P_p$) [kPa]; $\Delta\pi$ is the local bulk osmotic pressure difference between the feed and permeate ($\pi_f - \pi_p$) [kPa]; and A_m is the membrane surface area [m^2]. β is a streamwise average dimensionless correction factor which can account for concentration polarization effects and also, as seen later, nonlinearities in the osmotic pressure function. When neither effect is present, $\beta = 1$.

Using van 't Hoff's equation for osmotic pressure

$$\Delta\pi = \pi_f - \pi_p = C\left(w_f - w_p\right) \quad (2)$$

where w is the bulk stream salinity (mass of solutes per unit mass of solution) [g/kg] and C is a modified van 't Hoff coefficient [kPa-kg/g] (see Appendix Section A.1; nonlinearities in osmotic pressure are considered in detail in a later section). Therefore,

$$d\dot{m}_p = A\left[\Delta P - \beta \cdot C\left(w_f - w_p\right)\right]dA_m \quad (3)$$

Conservation of solutes is applied for the feed side between the inlet and an arbitrary location along the flow channel:

$$\dot{m}_{s,f} = \dot{m}_{f,in} \times w_{f,in} = \dot{m}_f \times w_f \quad (4)$$

[3] The water permeability coefficient (A) is often given in units of m/s-bar or L/m^2-hr-bar [12], which is the permeate water volume flux per unit pressure difference; however, for the present model, we express this coefficient on a mass basis (equivalent to multiplying it by the density of pure water and some SI conversion factors).

At the same arbitrary location, conservation of mass requires that

$$\dot{m}_{f,in} = \dot{m}_f + \dot{m}_p \tag{5}$$

Substitution of Eq. (5) into Eq. (4) yields

$$w_f = \frac{\dot{m}_{f,in} \times w_{f,in}}{\dot{m}_{f,in} - \dot{m}_p} \tag{6}$$

Under the assumed condition of 100% salt rejection, only pure water permeates though the membrane; hence the salinity and osmotic pressure of the permeate are zeros. Substituting Eq. (6) into Eq. (3) and setting $w_p = 0$ yields

$$d\dot{m}_p = A\left[\Delta P - \beta\left(C\frac{\dot{m}_{f,in} \times w_{f,in}}{\dot{m}_{f,in} - \dot{m}_p}\right)\right] dA_m \tag{7}$$

We now proceed to cast Eq. (7) in a dimensionless form. Three dimensionless parameters are introduced for this purpose.

Recovery ratio, *RR*

$$RR \equiv \frac{\dot{m}_p}{\dot{m}_{f,in}} \tag{8}$$

The recovery ratio is a primary performance metric of an RO mass exchanger as it represents the amount of pure water recovered from the feed stream. In so far as the inlet mass flow rate is greater than the maximum amount of permeate that can be recovered, the recovery ratio should not be confused with the effectiveness which will be described in the next section.

Osmotic pressure ratio, *SR*

$$SR_f \equiv \frac{\pi_{f,in}}{\Delta P} \tag{9}$$

The osmotic pressure ratio is the ratio of the osmotic pressure at the feed inlet to the trans-membrane hydraulic pressure difference. This ratio should always be less than one since the hydraulic pressure difference must be greater than the feed osmotic pressure during RO operation.

Mass Transfer Units, *MTU*

$$MTU \equiv \frac{AA_m \Delta P}{\dot{m}_{f,in}} \tag{10}$$

The number of mass transfer units (MTU) is a dimensionless parameter for a membrane mass exchanger similar to the number of transfer units (NTU) used in heat exchanger design. The total membrane area, A_m, is analogous to the total heat exchanger surface area; and A is the water permeability coefficient, which is analogous to the overall heat transfer coefficient in heat exchangers. The MTU parameter in this membrane-based mass exchanger plays the same role that NTU plays in ε-NTU analysis of heat exchangers.

Dividing Eq. (7) by $\dot{m}_{f,in}$ and substituting Eqs. (8-10) yields

$$dRR = \left(1 - \frac{\beta \cdot SR_f}{1-RR}\right) dMTU \tag{11}$$

With the boundary condition that $RR = 0$ when $MTU = 0$ (at the inlet), Eq. (11) can be integrated to give the mass transfer units MTU as follows

$$MTU = RR + SR'_f \ln\left(\frac{SR'_f - 1}{SR'_f + RR - 1}\right) \tag{12}$$

where SR'_f is a modified osmotic pressure ratio defined as

$$SR'_f \equiv \beta \cdot SR_f \tag{13}$$

Alternatively, an explicit solution for the recovery ratio can be obtained from Eq. (12) as follows

$$RR = 1 - SR_f' - SR_f'\omega\left[\left(\frac{1-SR_f'}{SR_f'}\right)\exp\left(\frac{1-SR_f'-MTU}{SR_f'}\right)\right] \quad (14)$$

where ω is the Lambert, or omega, function in which $\omega(x)$ is the solution to $x = \omega e^{\omega}$. Equation (12) can be used to calculate the required mass transfer units (hence the effective membrane surface area) of an RO mass exchanger since it is an explicit relation of the form

$$MTU = f(RR, SR_f, \beta) \quad (15)$$

Figure 3 shows the variation of the recovery ratio RR with mass transfer units MTU for varying osmotic pressure ratios at a temperature of 25 °C and neglecting the effects of concentration polarization and the nonlinearity of osmotic pressure (i.e., assuming $\beta = 1$). It is clear from Eq. (15) and from the asymptotic nature of the osmotic pressure ratio contours in Fig. 3 that the three dimensionless parameters are similar to effectiveness-NTU representations of heat exchangers in which NTU is a function of the effectiveness and the heat capacity rate ratio. However, additional derivation is needed to reach a parameter analogous to effectiveness. This will be developed in the next section.

3. RO Effectiveness

The effectiveness of the RO system can be defined as the ratio of the permeate flow rate actually achieved by an exchanger of a given size to the maximum possible permeate flow rate for a given hydraulic pressure and inlet osmotic pressure. The effectiveness, so defined, is the same as the ratio of the actual recovery ratio to the maximum possible recovery ratio. This definition is evident in Fig. 3, where the recovery ratio reaches a

maximum value for a given osmotic pressure ratio as the MTU becomes large. The exchanger effectiveness approaches one in this thermodynamic limit.

In the present section, we wish to derive a relation for the maximum recovery ratio in order to write an equation for the effectiveness. We note that the maximum permeate flow rate will be reached when the osmotic pressure difference between the feed and permeate rises to the point that the net driving potential ($\Delta P - \beta\Delta\pi$) equals zero at the outlet of the membrane channel. From Eq. (1), this fixes the outlet osmotic pressure

$$\Delta P = \beta\Delta\pi = \beta\pi_{f,out} \tag{16}$$

The relation between the inlet and outlet osmotic pressure can be obtained using conservation of solution and solute on the feed stream as follows

$$\pi_{f,out} = \frac{\pi_{f,in}}{1-RR} \tag{17}$$

Substituting Eq. (16) into Eq. (17), the following relation for the maximum recovery ratio is obtained

$$RR_{max} = 1 - SR_f' \tag{18}$$

Equation (18) gives the maximum recovery ratio as a function of the osmotic pressure ratio. Now, the effectiveness is defined as

$$\varepsilon \equiv \frac{RR}{RR_{max}} \tag{19}$$

Substituting Eq. (18) and (19) into Eq. (12), an expression for MTU as a function of the effectiveness can be obtained as given in Eq. (20):

$$MTU = \varepsilon\left(1 - SR_f'\right) - SR_f' \ln(1-\varepsilon) \tag{20}$$

Figure 4 shows the variation of effectiveness with the mass transfer units for contours of osmotic pressure ratio where $\beta = 1$. It may be observed that for small values of MTU, the effectiveness is approximately equal to MTU. This result can be found mathematically

from Eq. (20) by noting that $\ln(1-\varepsilon) \approx -\varepsilon$ for small values of ε. The result can also be found, as shown in Eq. (21), by substituting the integrated form of the zero-dimensional transport equation, Eq. (1), along with Eq. (18) into Eq. (19) while noting that $\Delta\pi \rightarrow \pi_{f,in}$ for a zero-dimensional exchanger with pure permeate:

$$\text{at } MTU \ll 1,\ \varepsilon = \frac{RR_{zero-dimensional}}{RR_{max}} = \frac{A \times A_m(\Delta P - \beta\Delta\pi)}{\dot{m}_{f,in}\left(1-\beta\frac{\pi_{f,in}}{\Delta P}\right)} = MTU \tag{21}$$

This is analogous to the well-known limit for heat exchangers where the effectiveness is equal to NTU as NTU approaches zero [47].

4. Determination of β via Numerical Model

The analytical solution given by Eqs. (12, 14, and 20) assumes a linear relationship between osmotic pressure and salinity. This assumption is acceptable for relatively dilute solutions, but for a high salinity feed the relationship between the osmotic pressure and salinity is somewhat nonlinear (See Appendix A.2). The analytical expressions also use a dimensionless parameter, β, to correct for deviations in performance resulting from feed-side external concentration polarization. In this section, a numerical model of a one-dimensional reverse osmosis mass exchanger is developed using a nonlinear function for the osmotic pressure, so as to determine the value of β for representative values of RO operation. The model applies a discretized form of the transport equation in one-dimension, and conservation of solutes and solvent to *N* membrane elements in series. The zero-dimensional transport equation used in the numerical model, Eq. (22), assumes that the permeate stream is pure and includes a feed-side external concentration polarization modulus where *k* is the mass transfer coefficient in m/s [25, 48].

$$\dot{m}_p = A\left[\Delta P - \pi_f \exp\left(\frac{\dot{m}_p}{k\cdot\rho_p\cdot A_m}\right)\right]A_m \quad (22)$$

The equations comprised by the numerical model were solved using Engineering Equation Solver [49], a simultaneous equation solver which iteratively solves sets of coupled nonlinear algebraic equations. The number of elements (differential control volumes) was increased to 50 at which point the results were seen to be grid independent. The total amount of permeate was calculated by numerically integrating the permeate mass flow rate produced by all elements. The development of the nonlinear osmotic pressure function used in this numerical model is given in the Appendix.

The numerical model is used to determine the deviations in the analytical model which result from the effects of concentration polarization and the use of a linearized osmotic pressure function. It is also used to determine representative values of β. All other assumptions made for the analytical model are also made for the numerical model. An additional assumption is that the RO membranes can withstand arbitrary net driving pressures. Two cases are considered and presented graphically: a brackish water case, $w_{f,in} = 5$ g/kg; and a seawater case, $w_{f,in} = 35$ g/kg. Two additional salinities are considered for calculating β: a concentrated wastewater stream, $w_{f,in} = 15$ g/kg; and a concentrated seawater stream, $w_{f,in} = 45$ g/kg.

The input parameters for the numerical calculation are given in Table 1. The water permeability coefficient used is representative of a typical spiral wound seawater membrane [46]. Mass transfer coefficients are highly dependent on the spacer geometry unique to each RO membrane module used. A representative value of the mass transfer coefficient for a spiral wound RO module was found to be $k = 3\times10^{-5}$ m/s using parameters found in [23]. To produce a representative k it is assumed that the flow within

the feed channel is fully developed and k was held at a constant [average] value throughout the length of the exchanger. A ten percent increase or decrease in k yielded a maximum deviation in recovery ratio of about 4.5% for the concentrated seawater case, $w_{f,\,in}$ = 45 g/kg, where SR_f = 0.3 and MTU << 1.

Values of β for each of the four inlet salinities are determined by equating the analytical and numerical model recovery ratios and solving for β. For brackish and seawater feed salinities, β is plotted versus MTU for contours of osmotic pressure ratio as shown in Figs. 5 and 6. Tables 2 – 5 display β for all four salinities as a function of SR_f and MTU using inputs given in Table 1. For seawater and concentrated seawater feed salinities, the recovery ratios would yield unphysical conditions for SR_f = 0.1 and 0.2, so these cases are excluded. In certain cases, β may be less than unity because of the deviation in the linear and nonlinear osmotic pressure.

To determine the effectiveness from the numerical model, we once again note that the maximum recovery ratio, RR_{max}, is achieved when the equality from Eq. (16) holds. Applying conservation of solutes and solution to the feed stream yields the following expression:

$$RR_{max} = 1 - \frac{w_{f,in}}{w_{f,out,max}} \tag{23}$$

The maximum outlet salinity, $w_{f,out,max}$, is determined by Eq. (16) of which the osmotic pressure at the outlet, $\pi_{f,out}$, is a function. The effectiveness can now be determined by Eq. (17) using the maximum recovery ratio defined by Eq. (23).

5. Effect of Osmotic Pressure Nonlinearity and Concentration Polarization

In this section, we use the analytical and numerical models to show the effects of concentration polarization and nonlinearity in the osmotic pressure function.

a. Osmotic Pressure Nonlinearity

We first examine the deviation of the model's predictions for recovery ratio and effectiveness resulting from nonlinearity in osmotic pressure. For this comparison, the exponential concentration polarization modulus is not included in the numerical solution. Figure 7 shows the recovery ratio versus mass transfer units for varying osmotic pressure ratios. The black solid lines are the same curves displayed in Fig. 3, and the circles and triangles are for the brackish water and seawater cases using the nonlinear function for osmotic pressure. As shown in Fig. 7, the maximum deviation of the analytical result from the seawater numerical result is about 6.9% for $SR_f = 0.3$. This is because for a high salinity feed stream (i.e., the seawater case), and at higher recovery ratio (RR = 0.65 at this large deviation), the exit brine has a very high salinity, hence the actual osmotic pressure deviates significantly from the linear model. Because the actual osmotic pressure is higher than the linearized pressure at high salinities (see Fig. A1 in Appendix), the amount of permeate is reduced and the maximum achievable recovery ratio declines. The maximum recovery ratio achievable also decreases when the nonlinear osmotic pressure is applied because the thermodynamic performance limit is a function of the outlet feed salinity. These linearization errors may be reduced by using a modified van't Hoff coefficient fitted to the osmotic pressure range of interest.

Deviations in recovery ratio for the brackish water case do not exceed 2% from the analytical model. This is because the osmotic pressure is nearly linear with salinity for low salinity feeds such as brackish water and municipal wastewater.

Figure 8 shows the effectiveness as a function of MTU varying with osmotic pressure ratios for both the analytical and numerical cases. Again it is found that the greatest deviation associated with linearization is for high salinity feed solutions and low osmotic pressure ratios. For the seawater case, a maximum deviation of 6.5% was found for an osmotic pressure ratio of 0.3. For the brackish water case, a maximum deviation of 1% was found.

b. Concentration Polarization

Figure 9 displays the recovery ratio versus MTU for brackish water, $w_{f,\,in}$ = 5 g/kg, and 4 cases of mass transfer coefficient: k = 3x10^{-6}, 3x10^{-5}, 3x10^{-4} m/s, and $k \rightarrow \infty$ m/s. The fourth case ($k \rightarrow \infty$) represents a system that has no concentration polarization but which includes the effect of osmotic pressure nonlinearity. Figure 9 shows that smaller values of k and SR_f exacerbate the effect of concentration polarization on performance. Nondimensionalizing the exponential CP modulus from Eq. (22) for a zero-dimensional exchanger predicts this effect:

$$\exp\left(\frac{\dot{m}_p}{k\cdot\rho_p\cdot A_m}\right) = \exp\left(\frac{RR}{MTU}\frac{1}{SR_f}\frac{\pi_{f,in}A}{k\cdot\rho_p}\right) \tag{24}$$

Looking at Eq. (24), we would expect that a higher feed salinity, i.e. higher inlet feed osmotic pressure, would likewise lead to a greater reduction in performance due to CP effects.

Figure 10 displays the recovery ratio versus MTU for 4 cases of k for a seawater feed salinity, $w_{f,\,in}$ = 35 g/kg. Comparing Figs. 9 and 10, it can be seen that the brackish water case experiences less performance reduction due to concentration polarization than in the seawater case. Also, both figures show that for the membrane permeability coefficient chosen, a mass transfer coefficient less than $3\text{x}10^{-5}$ m/s can lead to a steep reduction in attainable performance. Finally, both figures illustrate how the presence of CP requires more membrane area to achieve the same recovery ratio attainable with an ideal RO exchanger without CP. For example, the maximum recovery ratio is 0.47 at MTU = 5 for the seawater SR_f = 0.5 and k = 3 $\text{x}10^{-5}$ m/s contour whereas the RO exchanger without CP, represented by the $k \to \infty$ contour, achieves the same recovery ratio at MTU = 3.23. Calculating the membrane area required using the parameters from Table 1, CP effects result in an increase from 173 m^2 to 268 m^2, a nearly 55% increase.

6. Comparison to Literature Data

In order to validate the present work, we compare the numerical model results to experimental data collected by [33, 50-52]. In these experiments, a solution of sodium chloride is used as the feed solution. The mass transfer coefficient for each experimental run is calculated by [25]:

$$k = 0.01625 \times \text{Re}^{0.875}\text{Sc}^{0.25}\frac{D}{h} \tag{25}$$

For simplicity, the mass transfer coefficient is considered to be an average value and is held as constant throughout the exchanger. The average Reynolds number is calculated as:

$$\text{Re} = \frac{4h\dot{m}_{f,mean}}{\rho_{f,in}A_c\nu} \tag{26}$$

In the above equations, h is half of the feed channel height, the Schmidt number Sc is the mass diffusivity D divided by the kinematic viscosity ν, and A_c is the feed channel cross sectional area (membrane width times feed channel height). In some cases the membrane width was determined by dividing the membrane area A_m by the membrane length. The osmotic pressure for aqueous NaCl was calculated from Eq. (A.4) with the osmotic coefficient ϕ provided by [53].

Figure 11 shows the measured recovery ratio versus the calculated recovery ratio using the present numerical model. It is apparent that the model predicts some data sets better than others. The data for which the model shows good agreement are: Van Wagner et al. [50], who used NaCl and coupon sized membranes; Song et al. [33], who used NaCl and spiral wound RO modules; and the low salt passage data from Prabhakar et al. [51] data, who used NaCl and two different cellulose acetate membranes one of which had low salt passage (SP) (~10%) and another which had high SP (~50%). Salt passage is defined as the ratio of the module outlet product salinity to the inlet feed salinity. Data which the model does not predict well were those associated with high SP membranes [51] because salt passage was not included in the present model. It must also be noted that a membrane length was not reported in [51]; however, applying several guessed values spanning from 0.1 m to 10 m resulted in less than 1.3% change in mean error.

The maximum and mean error across all data, with the exception of the high salt passage data [51], is 29.3% and 7.8%, respectively. The range of independent variables spanned by the validation is: 6.35E-4 < MTU < 1.78; 5.21×10^{-4} < RR < 0.96; 0.0105 < SR_f < 0.416; 1.19×10^{-6} < k [m/s] < 1.81×10^{-4}; 1.0 < β < 1.93. The average k value calculated across all data sets was 1.93×10^{-5} m/s.

7. Conclusions

The major conclusions of this paper are as follows:

- A closed form analytical solution for a one-dimensional reverse osmosis mass exchanger was developed. The equation expresses the recovery ratio of the membrane as a function of two dimensionless groups: the osmotic pressure ratio and the number of mass transfer units. A correction factor is introduced into the model to allow for the effects of concentration polarization and nonlinearity in the osmotic pressure as a function of salinity.
- A robust analogy exists between heat exchangers and osmotic mass exchangers in which the effectiveness can be expressed by four dimensionless groups. This novel ε-MTU model developed for the osmotic mass exchanger can be used to size or rate RO systems.
- The present model can be used to quantify the effects of feed-side external concentration polarization and nonlinearity in the osmotic pressure function on recovery ratio. The model can be used to estimate the amount of additional membrane area required to provide the same recovery ratio achievable by an ideal RO exchanger, provided the recovery ratio is at or equal to the maximum recovery ratio attainable by the exchanger.
- A mean error of 7.8% was found by comparing sets of experimentally obtained recovery ratios from appropriate literature sources and recovery ratios calculated from the present model.

Acknowledgments

The authors would like to thank King Fahd University of Petroleum and Minerals in Dhahran, Saudi Arabia, for funding the research reported in this paper through the Center for Clean Water and Clean Energy at MIT and KFUPM.

Appendix

A.1 Modified van 't Hoff Coefficient

The van 't Hoff equation [53] applies to dilute, ideal solutions and is given as:

$$\pi \approx iRTc \tag{A.1}$$

where i is the van 't Hoff factor, R is the universal gas constant, T is the absolute temperature, and c is the molarity of the solution with units of mol solvent/m^3 solution. Molarity can be expressed as a function of salinity, the density of the solution, and the molecular weight of the solute in units of g/mol:

$$c = \frac{\rho_{solution} w}{M_{solute}} \tag{A.2}$$

Because the van 't Hoff equation assumes a dilute solution, the density in Eq. (A.2) is approximated as that of pure water. Substituting this expression for molarity into the van 't Hoff equation Eq. (A.1), we can now define a modified van 't Hoff coefficient, C, to linearize the osmotic pressure function:

$$\pi \approx \frac{iRT\rho_{pure}}{M_{solute}} w = Cw \tag{A.3}$$

Using a least squares method, the modified van 't Hoff coefficient (C) is determined to be 73.45 kPa-kg/g at $T = 25^{o}$C for a solution in which the solutes are in the same mass proportion as in seawater. This linear model represented by Eq. (A.3) can be used for a salinity range of 0 to 70 g/kg, which is the typical range for most desalination applications. For this range, the maximum deviation from the non-linear osmotic pressure function (see section A.2) is 6.8%.

A.2 Derivation of Nonlinear Osmotic Pressure Function

From Robinson and Stokes [53], the osmotic pressure for a solution composed of multiple solutes can be written as:

$$\pi = \phi(RT\rho_{solvent})\sum_{j=solutes} b_j \tag{A.4}$$

where ϕ is the osmotic coefficient; R is the universal gas constant; $\rho_{solvent}$ is the density of the solvent, in this case pure water; and b_j is the molality of the jth solute in the solution. The molality of a solution [kg/kg-solvent] written as a function of salinity is

$$\sum_{j=solutes} b_j = \frac{1}{(1-w)}\sum_j \frac{w_j}{M_j} \tag{A.5}$$

where w is the salinity of the solution, w_j is the salinity of the j^{th} solute, and M_j is the molar mass of the j^{th} solute with units of kg/mol. A table of seawater constituents, which we will call a recipe, is provided by Millero and Leung [54] where the salinity for each solute of seawater, w_j, is given for a solution of a fixed salinity, w. To use the recipe, we note that w_j can be scaled with a solution of variable salinity, w, by the following expression:

$$w_j = \frac{w \cdot w_{j,recipe}}{\sum_j w_{j,recipe}} \tag{A.6}$$

This scaling is substituted into Eq. (A.5) giving

$$\sum_{j=solutes} b_j = \frac{w}{(1-w)}\sum_j \frac{w_{j,recipe}}{M_j \sum_j w_{j,recipe}} \tag{A.7}$$

Using the seawater recipe, the summed term on the right side of Eq. (A.7) results in a value of 31.841 mol/kg-solvent.

A correlation for the osmotic coefficient of seawater is given by Sharqawy *et al.* [55] and is valid between 0 and 200^{o}C and for salinities between 10 and 120 g/kg. The osmotic coefficient for a mixture, as described by Debye-Hückel theory, approaches a

value of 1 with decreasing salinity and does so independently of temperature. Literature values and correlations of the osmotic coefficient and osmotic pressure for diluted seawater with a salinity of 10 g/kg and below which adhere to this proper physical limit are difficult to find. Therefore, an extension of the correlation provided by Sharqawy *et al.* [55] is proposed by use of the theoretical expression for the osmotic coefficient given in Eq. (A.8), Brønsted's equation [56]:

$$\phi = 1 - \kappa\sqrt{b} + \lambda b \tag{A.8}$$

This expression is dependent on two constants, κ and λ. To find the value of these constants, Eq. (A.5) and its first derivative with respect to salinity are set to equal the value of ϕ given by the correlation and its first derivative with respect to salinity at a salinity of 10 g/kg, forming two equations with the two constants as unknowns. At 25^{o}C, the two constants are found to be κ = 0.3484 and λ = 0.3076. The final osmotic coefficient function is now set to be a piece-wise function with Eq. (A.5) forming the function for 0 $\leq w <$ 10 g/kg and the correlation forming the 10 $\leq w \leq$ 120 g/kg section. The extended osmotic coefficient function and the sum of molalities as a function of salinity, Eq. (A.4), provide the osmotic pressure of a stream at a given temperature and salinity. The osmotic coefficient, nonlinear osmotic pressure, and linear osmotic pressure are shown as a function of salinity in Fig. (A.1).

References

[1] U. Merten, Desalination By Reverse Osmosis, MIT Press, Cambridge, MA, 1966.
[2] H.K. Lonsdale, Recent advances in reverse osmosis membranes, Desalination, 13 (1973) 317-332.
[3] K.C. Channabasappa, Status of reverse osmosis desalination technology, Desalination, 17 (1975) 69-73.
[4] G. Jonsson, Overview of theories for water and solute transport in UF/RO membranes, Desalination, 35 (1980) 21-38.
[5] D.E. Potts, R.C. Ahlert, S.S. Wang, A critical review of fouling of reverse osmosis membranes, Desalination, 36 (1981) 235-264.
[6] E.A. Mason, H.K. Lonsdale, Statistical-mechanical theory of membrane transport, Journal of Membrane Science, 51 (1990) 1-81.
[7] J.G. Wijmans, R.W. Baker, The solution-diffusion model: a review, Journal of Membrane Science, 107 (1995) 1-21.
[8] K. Jamal, M.A. Khan, M. Kamil, Mathematical modeling of reverse osmosis systems, Desalination, 160 (2004) 29-42.
[9] C. Fritzmann, J. Löwenberg, T. Wintgens, T. Melin, State-of-the-art of reverse osmosis desalination, Desalination, 216 (2007) 1-76.
[10] H. Strathmann, Membrane separation processes, Journal of Membrane Science, 9 (1981) 121-189.
[11] H.K. Lonsdale, The growth of membrane technology, Journal of Membrane Science, 10 (1982) 81-181.
[12] O. Kedem, A. Katchalsky, Thermodynamic analysis of the permeability of biological membranes to non-electrolytes, Biochimica et Biophysica Acta, 27 (1958) 229-246.
[13] K.S. Spiegler, O. Kedem, Thermodynamics of hyperfiltration (reverse osmosis): criteria for efficient membranes, Desalination, 1 (1966) 311-326.
[14] D. Van Gauwbergen, J. Baeyens, Modelling reverse osmosis by irreversible thermodynamics, Separation and Purification Technology, 13 (1998) 117-128.
[15] A. Katchalsky, O. Kedem, Thermodynamics of Flow Processes in Biological Systems, Biophysical Journal, 2 (1962) 53-78.
[16] S. Tanimura, S.-i. Nakao, S. Kimura, Transport equation for a membrane based on a frictional model, Journal of Membrane Science, 84 (1993) 79-91.
[17] H.K. Lonsdale, U. Merten, R.L. Riley, Transport properties of cellulose acetate osmotic membranes, Journal of Applied Polymer Science, 9 (1965) 1341-1362.
[18] D.R. Paul, Reformulation of the solution-diffusion theory of reverse osmosis, Journal of Membrane Science, 241 (2004) 371-386.
[19] P. Mukherjee, A.K. SenGupta, Some observations about electrolyte permeation mechanism through reverse osmosis and nanofiltration membranes, Journal of Membrane Science, 278 (2006) 301-307.
[20] G. Mauviel, J. Berthiaud, C. Vallieres, D. Roizard, E. Favre, Dense membrane permeation: From the limitations of the permeability concept back to the solution-diffusion model, Journal of Membrane Science, 266 (2005) 62-67.

[21] A. Yaroshchuk, Influence of osmosis on the diffusion from concentrated solutions through composite/asymmetric membranes: Theoretical analysis, Journal of Membrane Science, 355 (2010) 98-103.
[22] E. Nagy, 1 - On Mass Transport Through a Membrane Layer, in: Basic Equations of the Mass Transport through a Membrane Layer, Elsevier, Oxford, 2012, pp. 1-34.
[23] E. Lyster, Y. Cohen, Numerical study of concentration polarization in a rectangular reverse osmosis membrane channel: Permeate flux variation and hydrodynamic end effects, Journal of Membrane Science, 303 (2007) 140-153.
[24] S.S. Sablani, M.F.A. Goosen, R. Al-Belushi, M. Wilf, Concentration polarization in ultrafiltration and reverse osmosis: a critical review, Desalination, 141 (2001) 269-289.
[25] L. Song, C. Liu, A total salt balance model for concentration polarization in crossflow reverse osmosis channels with shear flow, Journal of Membrane Science, 401–402 (2012) 313-322.
[26] H.-J. Oh, T.-M. Hwang, S. Lee, A simplified simulation model of RO systems for seawater desalination, Desalination, 238 (2009) 128-139.
[27] A. Matin, G. Ozaydin-Ince, Z. Khan, S.M.J. Zaidi, K. Gleason, D. Eggenspiler, Random copolymer films as potential antifouling coatings for reverse osmosis membranes, Desalination and Water Treatment, 34 (2011) 100-105.
[28] S. Sundaramoorthy, G. Srinivasan, D.V.R. Murthy, An analytical model for spiral wound reverse osmosis membrane modules: Part I — Model development and parameter estimation, Desalination, 280 (2011) 403-411.
[29] A. Chatterjee, A. Ahluwalia, S. Senthilmurugan, S.K. Gupta, Modeling of a radial flow hollow fiber module and estimation of model parameters using numerical techniques, Journal of Membrane Science, 236 (2004) 1-16.
[30] M.G. Marcovecchio, N.J. Scenna, P.A. Aguirre, Improvements of a hollow fiber reverse osmosis desalination model: Analysis of numerical results, Chemical Engineering Research and Design, 88 (2010) 789-802.
[31] M. Sekino, Precise analytical model of hollow fiber reverse osmosis modules, Journal of Membrane Science, 85 (1993) 241-252.
[32] C.S. Slater, J.M. Zielinski, R.G. Wendel, C.G. Uchrin, Modeling of small scale reverse osmosis systems, Desalination, 52 (1985) 267-284.
[33] L. Song, K.G. Tay, Performance prediction of a long crossflow reverse osmosis membrane channel, Journal of Membrane Science, 281 (2006) 163-169.
[34] M. Wilf, C. Bartels, Optimization of seawater RO systems design, Desalination, 173 (2005) 1-12.
[35] M. Li, Reducing specific energy consumption in Reverse Osmosis (RO) water desalination: An analysis from first principles, Desalination, 276 (2011) 128-135.
[36] M. Li, Optimal plant operation of brackish water reverse osmosis (BWRO) desalination, Desalination, 293 (2012) 61-68.
[37] M. Li, B. Noh, Validation of model-based optimization of brackish water reverse osmosis (BWRO) plant operation, Desalination, 304 (2012) 20-24.
[38] Y. Lu, A. Liao, Y. Hu, Optimization design of RO system for water purification, in: A.K. Iftekhar, S. Rajagopalan (Eds.) Computer Aided Chemical Engineering, Elsevier, 2012, pp. 230-234.

[39] M.H. Sharqawy, S.M. Zubair, J.H. Lienhard V, Second law analysis of reverse osmosis desalination plants: An alternative design using pressure retarded osmosis, Energy, 36 (2011) 6617-6626.
[40] M. Sorin, S. Jedrzejak, C. Bouchard, On maximum power of reverse osmosis separation processes, Desalination, 190 (2006) 212-220.
[41] A. Zhu, P.D. Christofides, Y. Cohen, Minimization of energy consumption for a two-pass membrane desalination: Effect of energy recovery, membrane rejection and retentate recycling, Journal of Membrane Science, 339 (2009) 126-137.
[42] A. Zhu, P.D. Christofides, Y. Cohen, On RO membrane and energy costs and associated incentives for future enhancements of membrane permeability, Journal of Membrane Science, 344 (2009) 1-5.
[43] A. Zhu, P.D. Christofides, Y. Cohen, Effect of Thermodynamic Restriction on Energy Cost Optimization of RO Membrane Water Desalination, Industrial & Engineering Chemistry Research, 48 (2008) 6010-6021.
[44] M.H. Sharqawy, L.D. Banchik, J.H. Lienhard V, Effectiveness–mass transfer units (ε–MTU) model of an ideal pressure retarded osmosis membrane mass exchanger, Journal of Membrane Science, 445 (2013) 211-219.
[45] W.M. Kays, A.L. London, Compact Heat Exchangers, 3rd ed., McGraw-Hill, New York, 1984.
[46] M. Wilf, Guidebook details membrane desalination technology, Balaban Desalination Publications, 2007.
[47] J.H. Lienhard IV, J.H. Lienhard V, A Heat Transfer Textbook, 3rd ed., Phlogiston Press, Cambridge, MA, 2008.
[48] G. Schock, A. Miquel, Mass transfer and pressure loss in spiral wound modules, Desalination, 64 (1987) 339-352.
[49] S.A. Klein, Engineering Equation Solver, Academic Professional Version 9.214, in, http://www.fchart.com/. 2012.
[50] E.M. Van Wagner, A.C. Sagle, M.M. Sharma, B.D. Freeman, Effect of crossflow testing conditions, including feed pH and continuous feed filtration, on commercial reverse osmosis membrane performance, Journal of Membrane Science, 345 (2009) 97-109.
[51] S. Prabhakar, M.P.S. Ramani, A new concept of mass transfer coefficient in reverse osmosis — practical applications, Journal of Membrane Science, 86 (1994) 145-154.
[52] S. Sundaramoorthy, G. Srinivasan, D.V.R. Murthy, An analytical model for spiral wound reverse osmosis membrane modules: Part II — Experimental validation, Desalination, 277 (2011) 257-264.
[53] R.A. Robinson, R.H. Stokes, Electrolyte solutions, Dover Publications Inc., Mineola, New York, 2002.
[54] F.J. Millero, W.H. Leung, The thermodynamics of seawater at one atmosphere, American Journal of Science, 276 (1976) 1035–1077.
[55] M.H. Sharqawy, J.H. Lienhard V, S.M. Zubair, Thermophysical Properties of Sea Water: A Review of Existing Correlations and Data, Desalination and Water Treatment, 16 (2010) 354 – 380.
[56] K.S. Pitzer, Thermodynamics, 3rd ed., McGraw-Hill, New York, 1995.

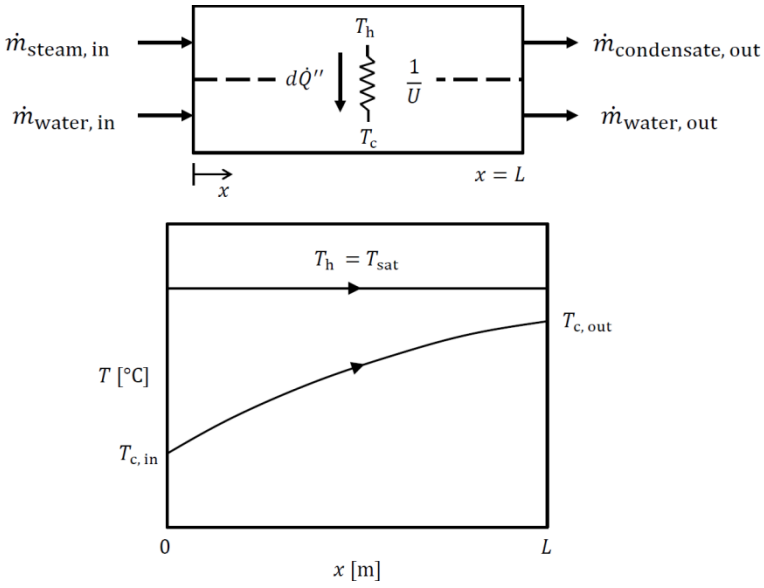

(a) Single-stream heat exchanger

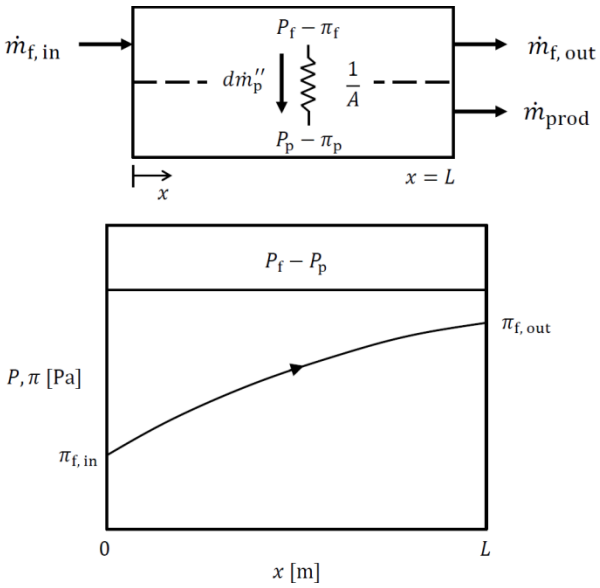

(b) Single-stream osmotic mass exchanger

Fig. 1 Temperature and pressure variations in a single-stream heat and osmotic mass exchanger.

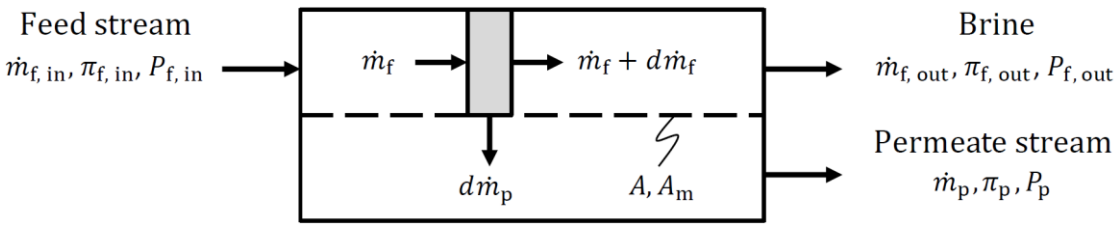

Fig. 2 Schematic drawing of a membrane-based RO mass exchanger.

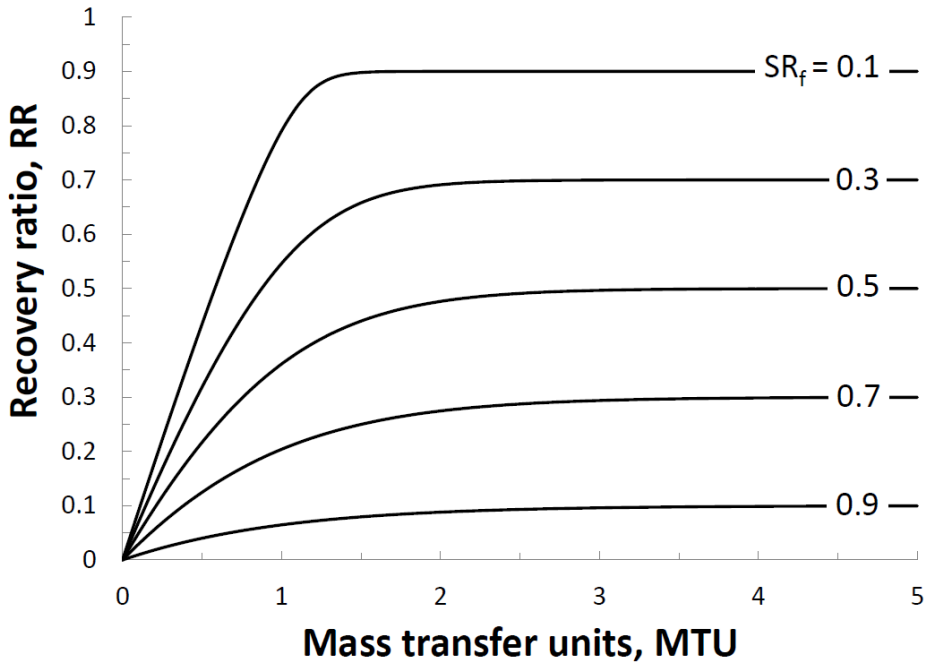

Fig. 3 Recovery ratio vs. mass transfer units for contours of osmotic pressure ratio. No correction for concentration polarization or nonlinearity in osmotic pressure is implemented ($\beta = 1$).

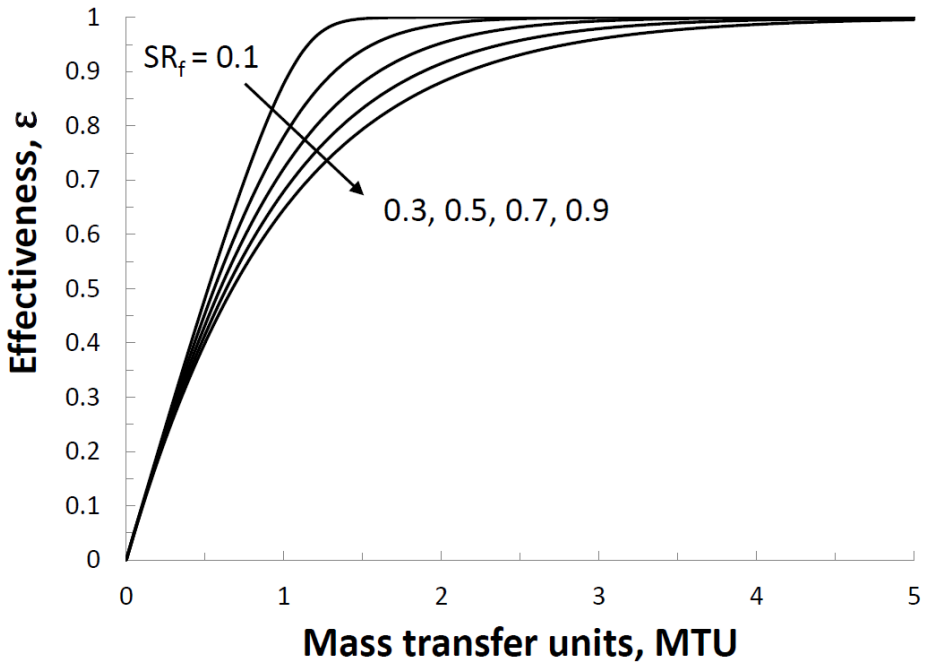

Fig. 4 Effectiveness vs. mass transfer units for contours of osmotic pressure ratio. No correction for concentration polarization or nonlinearity in osmotic pressure is implemented ($\beta = 1$).

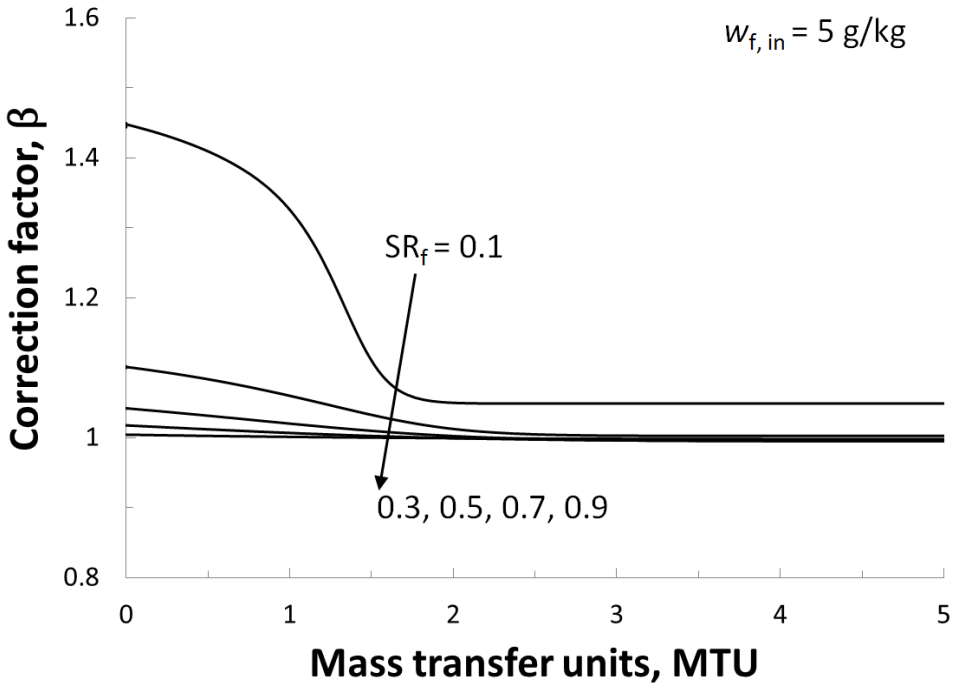

Fig. 5 Correction factor β vs. mass transfer units for varying osmotic pressure ratios, a feed inlet salinity representative of brackish water, and a representative mass transfer coefficient.

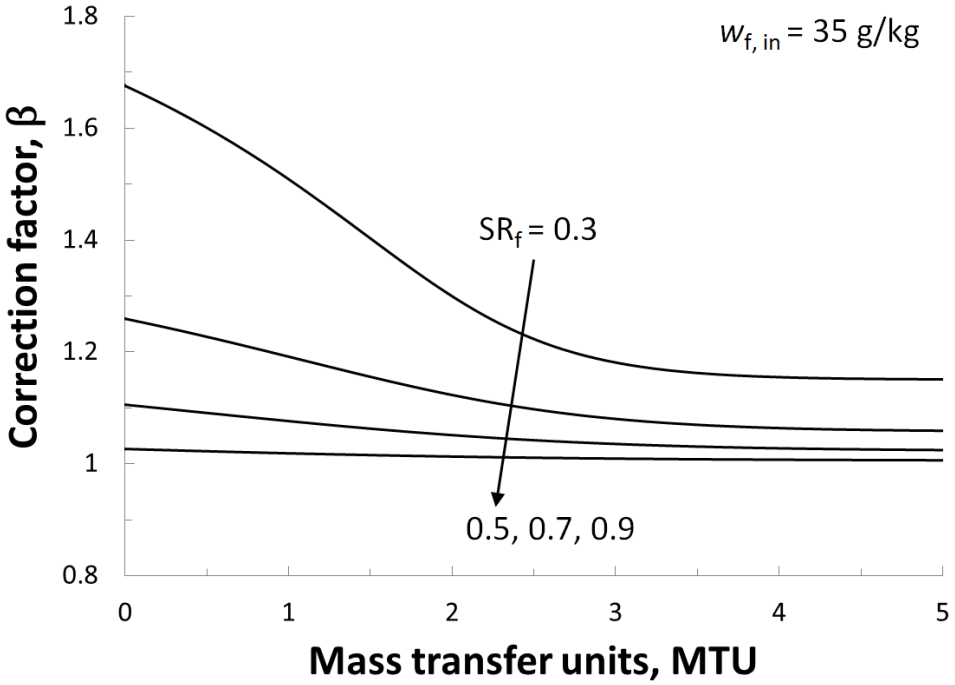

Fig. 6 Correction factor β vs. mass transfer units for varying osmotic pressure ratios, a feed inlet salinity representative of seawater, and a representative mass transfer coefficient.

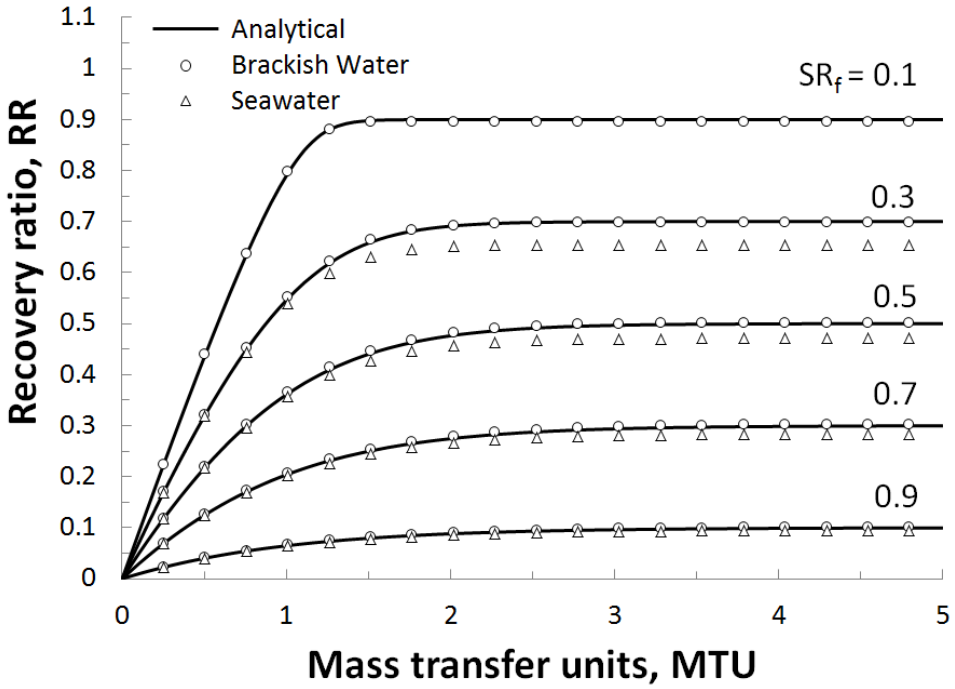

Fig. 7 Recovery ratio vs. mass transfer units with contours of osmotic pressure ratio for (1) analytical Eq. (13), (2) brackish water with a nonlinear osmotic pressure function, and (3) seawater with a nonlinear osmotic pressure function

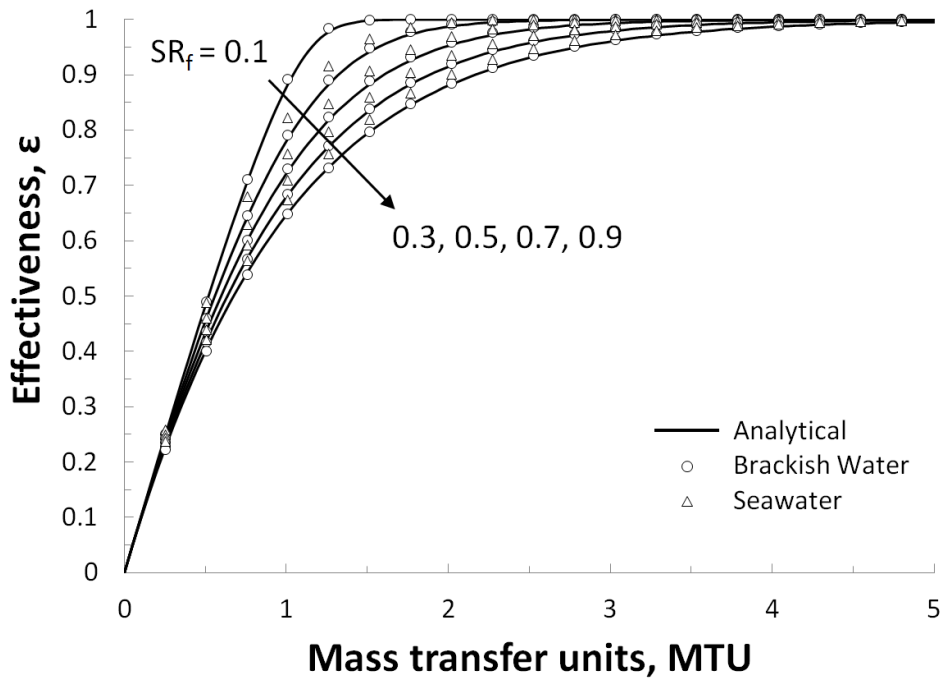

Fig. 8 Effectiveness factor vs. mass transfer units with contours of osmotic pressure ratio for (1) analytical Eq. (21), (2) brackish water with a nonlinear osmotic pressure function, (3) seawater with a nonlinear osmotic pressure function

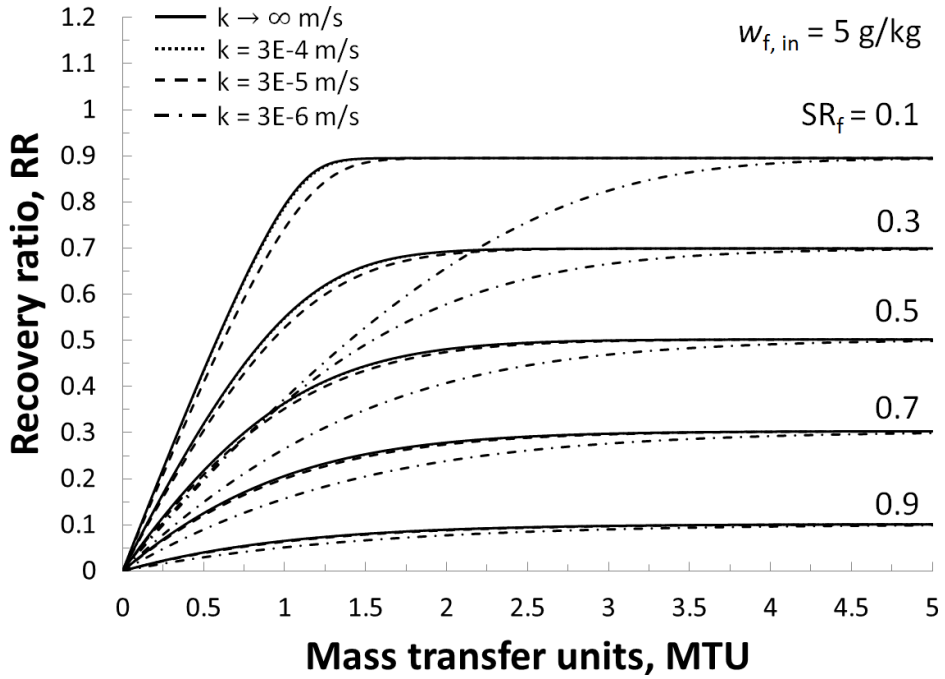

Fig. 9 Recovery ratio vs. mass transfer units with contours of osmotic pressure ratio for brackish water $w_{f,\,in}$ = 5 g/kg, and four values of mass transfer coefficient including the effects of concentration polarization and osmotic pressure nonlinearity.

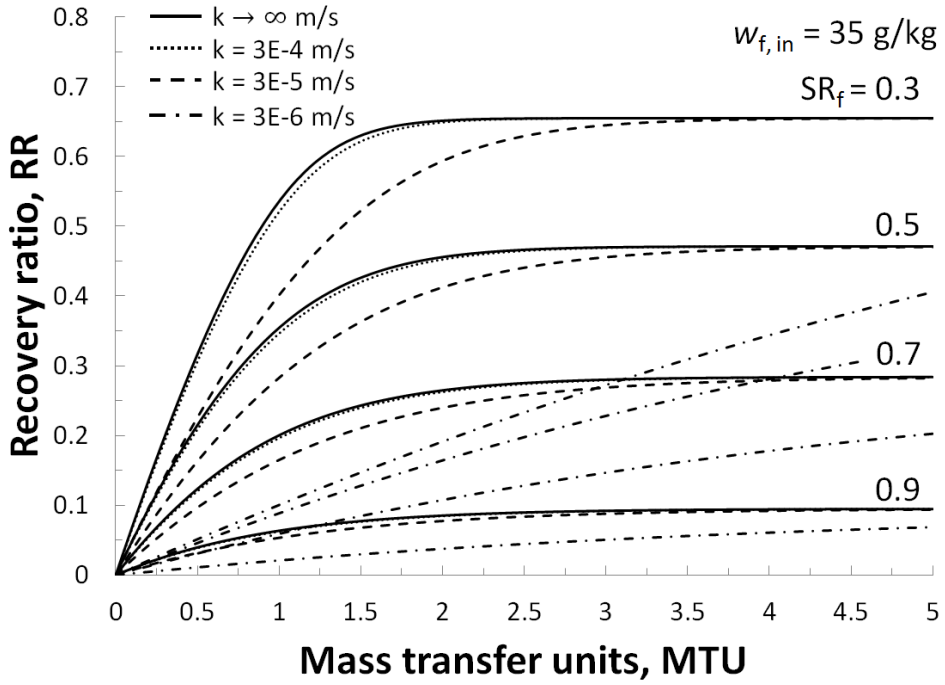

Fig. 10 Recovery ratio vs. mass transfer units with contours of osmotic pressure ratio for seawater $w_{f,in}$ = 35 g/kg, and four values of mass transfer coefficient including the effects of concentration polarization and osmotic pressure nonlinearity.

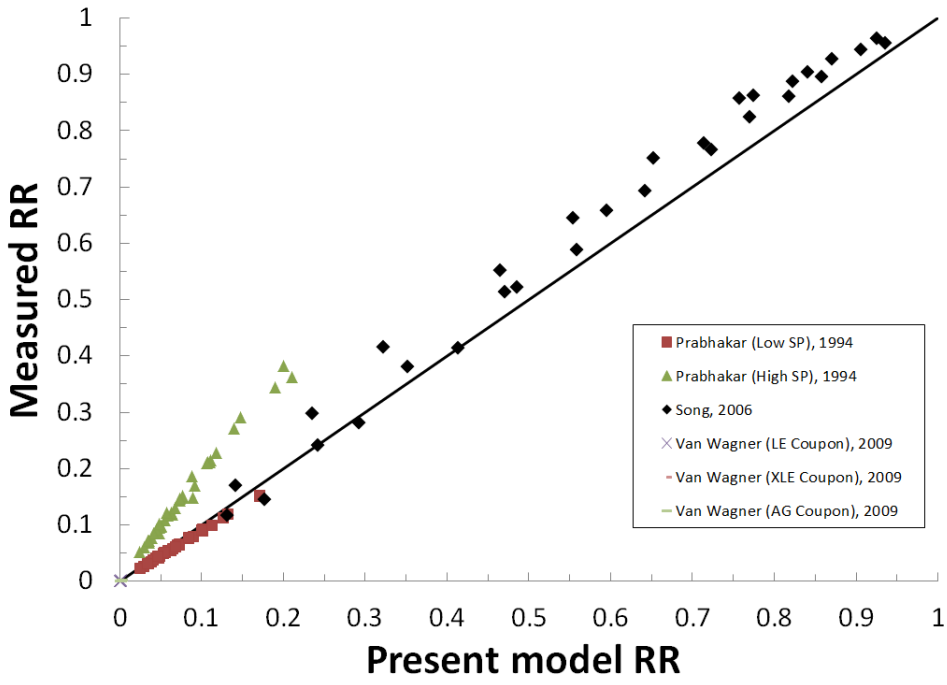

Fig. 11 Comparison of recovery ratios from measured empirical data and the present numerical model.

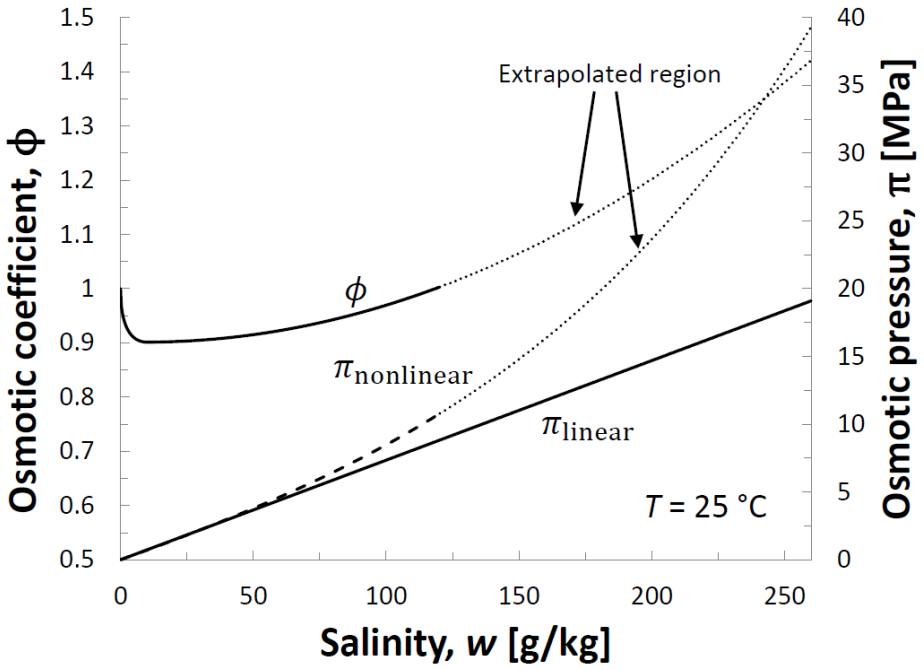

Fig. A.1 Seawater osmotic coefficient and osmotic pressures versus salinity for a fixed temperature shown as solid and dashed curves, respectively. The osmotic coefficient curve and nonlinear osmotic pressure curves are extrapolated for salinities greater than 120 g/kg and these sections are shown as bold dashed lines. The linear osmotic pressure curve is solid and bolded.

Table 1. Data input for numerical model

Input	Value / Range
Temperature, T	25 °C
Modified water permeability coefficient, A	3.61×10^{-6} kg/m^2-s-kPa
Feed mass flow rate, $\dot{m}_{f,in}$	1 kg/s
Inlet feed salinity, $w_{f,in}$	5, 15, 35, and 45 g/kg
Mass transfer coefficient, k	3×10^{-5} m/s
Trans-membrane pressure difference, ΔP	0.4 – 33.8 MPa
Membrane area, A_m	0 – 3.46×10^{3} m^2

Table 2. Correction factor for $w_{f,\,in}$ = 5 g/kg inlet salinity

MTU	β for indicated osmotic pressure ratios, $\pi_{f,in}/\Delta P$								
	0.1	0.2	0.3	0.4	0.5	0.6	0.7	0.8	0.9
0	1.448	1.180	1.101	1.064	1.042	1.028	1.018	1.010	1.005
0.2	1.435	1.172	1.095	1.059	1.038	1.025	1.016	1.009	1.004
0.4	1.419	1.162	1.088	1.053	1.034	1.022	1.013	1.008	1.003
0.6	1.399	1.150	1.080	1.047	1.030	1.019	1.011	1.006	1.003
0.8	1.370	1.136	1.070	1.041	1.025	1.015	1.009	1.005	1.002
1	1.326	1.118	1.060	1.034	1.021	1.012	1.007	1.004	1.001
1.2	1.255	1.097	1.049	1.028	1.016	1.009	1.005	1.003	1.001
1.4	1.155	1.072	1.038	1.021	1.012	1.007	1.004	1.002	1.001
1.6	1.080	1.049	1.028	1.016	1.008	1.004	1.002	1.001	1.000
1.8	1.056	1.031	1.019	1.011	1.005	1.002	1.001	1.000	1.000
2	1.050	1.021	1.013	1.007	1.003	1.001	1.000	0.999	1.000
2.2	1.049	1.016	1.009	1.004	1.001	0.999	0.999	0.999	0.999
2.4	1.049	1.014	1.006	1.002	0.999	0.998	0.998	0.998	0.999
2.6	1.049	1.013	1.004	1.000	0.998	0.997	0.997	0.998	0.999
2.8	1.049	1.013	1.004	1.000	0.997	0.996	0.997	0.998	0.999
3	1.049	1.013	1.003	0.999	0.997	0.996	0.997	0.998	0.999
3.2	1.049	1.013	1.003	0.999	0.996	0.996	0.996	0.997	0.999
3.4	1.049	1.013	1.003	0.998	0.996	0.995	0.996	0.997	0.999
3.6	1.049	1.013	1.003	0.998	0.996	0.995	0.996	0.997	0.998
3.8	1.049	1.013	1.003	0.998	0.996	0.995	0.996	0.997	0.998
4	1.049	1.013	1.003	0.998	0.996	0.995	0.996	0.997	0.998
4.2	1.049	1.013	1.003	0.998	0.996	0.995	0.995	0.997	0.998
4.4	1.049	1.013	1.003	0.998	0.996	0.995	0.995	0.997	0.998
4.6	1.049	1.013	1.003	0.998	0.996	0.995	0.995	0.997	0.998
4.8	1.049	1.013	1.003	0.998	0.996	0.995	0.995	0.997	0.998
5	1.049	1.013	1.003	0.998	0.996	0.995	0.995	0.997	0.998

Table 3. Correction factor for $w_{f,\,in}$ = 15 g/kg inlet salinity

MTU	β for indicated osmotic pressure ratios, $\pi_{f,in}/\Delta P$								
	0.1	0.2	0.3	0.4	0.5	0.6	0.7	0.8	0.9
0	2.613	1.563	1.302	1.186	1.121	1.079	1.050	1.029	1.013
0.2	2.559	1.543	1.290	1.177	1.114	1.074	1.047	1.027	1.012
0.4	2.495	1.520	1.275	1.167	1.107	1.069	1.043	1.025	1.011
0.6	2.417	1.491	1.259	1.156	1.100	1.064	1.040	1.023	1.010
0.8	2.319	1.457	1.239	1.144	1.092	1.059	1.037	1.021	1.009
1	2.195	1.415	1.218	1.131	1.083	1.053	1.033	1.019	1.008
1.2	2.036	1.365	1.194	1.117	1.075	1.048	1.030	1.017	1.007
1.4	1.834	1.309	1.168	1.103	1.067	1.043	1.027	1.015	1.007
1.6	1.606	1.250	1.143	1.090	1.059	1.038	1.024	1.014	1.006
1.8	1.417	1.196	1.119	1.077	1.052	1.034	1.022	1.013	1.005
2	1.313	1.154	1.098	1.066	1.045	1.030	1.019	1.011	1.005
2.2	1.270	1.126	1.082	1.057	1.039	1.027	1.017	1.010	1.005
2.4	1.254	1.110	1.070	1.049	1.035	1.024	1.016	1.009	1.004
2.6	1.249	1.101	1.062	1.043	1.031	1.021	1.014	1.008	1.004
2.8	1.247	1.096	1.057	1.039	1.028	1.019	1.013	1.008	1.003
3	1.246	1.094	1.053	1.036	1.025	1.018	1.012	1.007	1.003
3.2	1.246	1.093	1.051	1.034	1.023	1.016	1.011	1.007	1.003
3.4	1.246	1.092	1.050	1.032	1.022	1.015	1.010	1.006	1.003
3.6	1.246	1.092	1.049	1.031	1.021	1.015	1.010	1.006	1.003
3.8	1.246	1.092	1.049	1.030	1.020	1.014	1.009	1.006	1.003
4	1.246	1.092	1.048	1.030	1.020	1.013	1.009	1.005	1.002
4.2	1.246	1.092	1.048	1.029	1.019	1.013	1.009	1.005	1.002
4.4	1.246	1.092	1.048	1.029	1.019	1.013	1.008	1.005	1.002
4.6	1.246	1.092	1.048	1.029	1.019	1.012	1.008	1.005	1.002
4.8	1.246	1.092	1.048	1.029	1.019	1.012	1.008	1.005	1.002
5	1.246	1.092	1.048	1.029	1.019	1.012	1.008	1.005	1.002

Table 4. Correction factor for $w_{f,in}$ = 35 g/kg inlet salinity

MTU	β for indicated osmotic pressure ratios, $\pi_{f,in}/\Delta P$						
	0.3	0.4	0.5	0.6	0.7	0.8	0.9
0	1.676	1.406	1.259	1.168	1.106	1.061	1.027
0.2	1.648	1.388	1.247	1.159	1.100	1.057	1.025
0.4	1.617	1.369	1.234	1.150	1.094	1.054	1.023
0.6	1.584	1.348	1.220	1.141	1.088	1.050	1.022
0.8	1.548	1.326	1.206	1.132	1.082	1.047	1.020
1	1.509	1.303	1.192	1.123	1.076	1.043	1.019
1.2	1.468	1.279	1.177	1.114	1.071	1.040	1.018
1.4	1.425	1.255	1.163	1.105	1.066	1.037	1.016
1.6	1.381	1.232	1.149	1.096	1.061	1.035	1.015
1.8	1.339	1.209	1.135	1.088	1.056	1.032	1.014
2	1.300	1.188	1.123	1.081	1.051	1.030	1.013
2.2	1.265	1.169	1.112	1.074	1.047	1.028	1.012
2.4	1.236	1.152	1.102	1.068	1.044	1.026	1.011
2.6	1.212	1.138	1.094	1.063	1.041	1.024	1.011
2.8	1.194	1.127	1.086	1.058	1.038	1.022	1.010
3	1.181	1.118	1.080	1.055	1.036	1.021	1.009
3.2	1.172	1.111	1.075	1.051	1.033	1.020	1.009
3.4	1.165	1.106	1.071	1.048	1.032	1.019	1.008
3.6	1.160	1.102	1.068	1.046	1.030	1.018	1.008
3.8	1.157	1.099	1.066	1.044	1.029	1.017	1.008
4	1.155	1.097	1.064	1.043	1.028	1.016	1.007
4.2	1.153	1.095	1.062	1.042	1.027	1.016	1.007
4.4	1.152	1.094	1.061	1.041	1.026	1.015	1.007
4.6	1.152	1.093	1.060	1.040	1.026	1.015	1.007
4.8	1.151	1.092	1.060	1.039	1.025	1.015	1.007
5	1.151	1.092	1.059	1.039	1.025	1.014	1.006

Table 5. Correction factor for $w_{f,\,in}$ = 45 g/kg inlet salinity

MTU	β for indicated osmotic pressure ratios, $\pi_{f,in}/\Delta P$						
	0.3	0.4	0.5	0.6	0.7	0.8	0.9
0	1.838	1.501	1.319	1.206	1.129	1.074	1.033
0.2	1.804	1.480	1.305	1.196	1.123	1.070	1.031
0.4	1.768	1.457	1.290	1.186	1.116	1.066	1.029
0.6	1.729	1.434	1.274	1.176	1.110	1.062	1.027
0.8	1.687	1.408	1.258	1.165	1.103	1.058	1.025
1	1.643	1.382	1.242	1.155	1.096	1.055	1.024
1.2	1.597	1.356	1.225	1.145	1.090	1.051	1.022
1.4	1.550	1.329	1.209	1.135	1.084	1.048	1.021
1.6	1.501	1.302	1.193	1.125	1.078	1.045	1.020
1.8	1.454	1.277	1.178	1.116	1.073	1.042	1.018
2	1.409	1.252	1.164	1.107	1.068	1.039	1.017
2.2	1.368	1.230	1.151	1.099	1.063	1.037	1.016
2.4	1.333	1.211	1.139	1.092	1.059	1.034	1.015
2.6	1.303	1.194	1.129	1.086	1.055	1.032	1.014
2.8	1.279	1.179	1.120	1.081	1.052	1.030	1.014
3	1.260	1.168	1.113	1.076	1.049	1.029	1.013
3.2	1.246	1.158	1.106	1.072	1.046	1.027	1.012
3.4	1.235	1.151	1.101	1.068	1.044	1.026	1.012
3.6	1.227	1.145	1.097	1.065	1.042	1.025	1.011
3.8	1.222	1.141	1.094	1.063	1.041	1.024	1.011
4	1.218	1.137	1.091	1.061	1.039	1.023	1.010
4.2	1.215	1.135	1.089	1.059	1.038	1.022	1.010
4.4	1.213	1.133	1.087	1.058	1.037	1.022	1.010
4.6	1.211	1.131	1.086	1.057	1.036	1.021	1.009
4.8	1.210	1.130	1.085	1.056	1.036	1.021	1.009
5	1.210	1.130	1.084	1.055	1.035	1.020	1.009